Characterization of Electronic and Ionic Transport in Li[subscript 1-x]Ni[subscript 0.33]Mn[subscript 0.33]Co[subscript 0.33]O[subscript 2](NMC[subscript 333]) and Li[subscript 1-x]Ni[subscript 0.50]Mn[subscript 0.20]Co[subscript 0.30]O[subscript 2](NMC[subscript 523]) as a Function of Li Content

Citation: Amin, Ruhul, and Chiang, Yet-Ming. "Characterization of Electronic and Ionic Transport in Li[subscript 1-x]Ni[subscript 0.33]Mn[subscript 0.33]Co[subscript 0.33]O[subscript 2] (NMC[subscript 333]) and Li[subscript 1-x]Ni[subscript 0.50]Mn[subscript 0.20]Co[subscript 0.30]O[subscript 2](NMC[subscript 523]) as a Function of Li Content." Journal of The Electrochemical Society 163, 8 (May 2016): A1512–A1517 © 2016 The Author(s)

As Published: http://dx.doi.org/10.1149/2.0131608JES

Publisher: Electrochemical Society

Persistent URL: http://hdl.handle.net/1721.1/111835

Version: Final published version: final published article, as it appeared in a journal, conference proceedings, or other formally published context

Characterization of Electronic and Ionic Transport in $Li_{1-x}Ni_{0.33}Mn_{0.33}Co_{0.33}O_2$ (NMC_{333}) and $Li_{1-x}Ni_{0.50}Mn_{0.20}Co_{0.30}O_2$ (NMC_{523}) as a Function of Li Content

Ruhul Amin[a,b] and Yet-Ming Chiang[a,z]

[a]*Department of Materials Science and Engineering, Massachusetts Institute of Technology (MIT), Cambridge, Massachusetts 02139, USA*
[b]*Qatar Environment and Energy Research Institute, Hamad Bin Khalifa University, Qatar Foundation, Doha, Qatar*

Despite the extensive commercial use of $Li_{1-x}Ni_{1-y-z}Mn_zCo_yO_2$ (NMC) as the positive electrode in Li-ion batteries, and its long research history, its fundamental transport properties are poorly understood. These properties are crucial for designing high energy density and high power Li-ion batteries. Here, the transport properties of NMC_{333} and NMC_{523} are investigated using impedance spectroscopy and DC polarization and depolarization techniques. The electronic conductivity is found to increase with decreasing Li-content (increasing state-of-charge) from $\sim 10^{-7}$ Scm^{-1} to $\sim 10^{-2}$ Scm^{-1} over Li concentrations $x = 0.00$ to 0.75, corresponding to an upper charge voltage of 4.8 V with respect to Li/Li^+. The lithium ion diffusivity is at least one order of magnitude lower, and decreases with increasing x to at $x = \sim 0.5$. The ionic conductivity and diffusivity obtained from the two measurements techniques (EIS and DC) are in good agreement, and chemical diffusion is limited by lithium transport over a wide state-of-charge range.
 [DOI: 10.1149/2.0131608jes]

Manuscript submitted December 31, 2015; revised manuscript received April 19, 2016. Published May 13, 2016.

Cathodes having high energy and power density, adequate safety, excellent cycle life, and low cost are a critical need for Li-ion batteries to enable the commercialization of electric transportation and stationary storage.[1] Towards this end, much previous research focused on the development of $LiNi_{1-x}Co_xO_2$ (NC)[2–10] cathode due to its high capacity (~275 mAh/g) and favorable operating cell voltage (4.3 V vs. Li/Li^+), which is within the voltage stability window of current liquid electrolytes, and lower cost than $LiCoO_2$. Despite extensive optimization, e.g., with respect to the Ni/Co ratio,[2–10] NC suffers from poor structural stability during electrochemical cycling.[11] Significant efforts were subsequently focused on improving structural stability and electrochemical performance by partial substitution Mn[12–17] (electrochemically inactive in this compound over the operating cell voltage window). Two of the most promising compositions that have emerged are $LiNi_{0.33}Mn_{0.33}Co_{0.33}O_2$ (NMC_{333}) and $LiNi_{0.50}Mn_{0.20}Co_{0.30}O_2$ (NMC_{523}), currently in widespread commercial use and development, respectively. This intercalation compound exhibits solid solution behavior during the extraction of lithium[3,4,18] and is structurally stable upon cycling.[12] There is also much current interest in extending the charge voltage window upwards to capture greater capacity and energy. However, there is surprisingly little, and conflicting, data on the basic transport properties of the NMC family of compounds.[19–23] Wu et al.,[19] and Hao[20] measured using the GITT technique the chemical diffusivity of NMC_{333} based composite electrodes (e.g., NMC powder combined with polymer binder and carbon additive) as a function of lithium content, and reported results differing by two orders of magnitude from each other. Furthermore, whereas Hao[20] reported that the chemical diffusivity of NMC_{333} is nearly independent of lithium content, Wu et al.[19] found two orders of magnitude variation of lithium diffusivity with lithium content. Gu et al.[21] and Li et al.[23] measured the lithium ion diffusivity of lithiated NMC_{333}, also in the form of composite electrodes, using cyclic voltammetry (CV). The results differed by four orders of magnitude between the two studies (10^{-14} cm^2/s vs. 10^{-10} cm^2/s). With respect to electronic conductivity, we know of no published measurements for NMC_{333} and NMC_{523} compositions. Seid et al.[22] reported that the electronic conductivity of $Li_{1.04}Ni^{2+}{}_{0.235}Ni^{3+}{}_{0.09}Mn^{4+}{}_{0.315}Co^{3+}{}_{0.32}O^2$ exhibits semiconductor-like behavior with a room temperature conductivity of $\sim 10^{-5}$ Scm^{-1}.

Thus our objective in this work is to systematically characterize and interpret the transport properties of NMC_{333} and NMC_{523}. We use additive-free, single phase sintered samples in which the extrinsic effects due to binders, conductive additives, and particle microstructures that may be present in composite electrodes are avoided. Using electron blocking and ionic blocking cell configurations, respectively, and electrochemical impedance spectroscopy and DC polarization and depolarization techniques (see Table I), we deconvolute the electronic and ionic conductivities of NMC_{333} and NMC_{523} as a function of temperature and Li content, up to a lithium deficiency of $x = 0.75$, which corresponds to high charge voltages of 4.7 V and 4.8 V for NMC_{333} and NMC_{523} respectively. Our sample configuration permits measurement of single-phase properties up to delithiation levels (state-of-charge) where electrochemically-induced microfracture intrudes. Electronic conductivity was not apparently affected by these effects, whereas ionic transport shows an apparent increase beyond $x = 0.50$ which we attribute to fast transport paths created by microfracture.

Experimental

NMC powder of $LiNi_{0.33}Mn_{0.33}Co_{0.33}O_2$ (NMC_{333}) and $LiNi_{0.50}Mn_{0.20}Co_{0.30}O_2$ (NMC_{523}) compositions were obtained from TODA America Inc. (Battle Creek, MI, USA). Compacted pellets were prepared from the powder by pressing at 340 MPa, forming cylindrical samples of 14 mm diameter. The pellets were sintered at 900°C for 12 h in ambient atmosphere, preceded by heating at 5°C/min, and followed by cooling at the same rate. This procedure yielded samples of 96–98% relative density, sufficiently high that the measured conductivity represents the bulk value. Corrections for porosity are small because for solids of high density, porosity reduces the effective cross-sectional area in direct proportion to the pore volume fraction, and the conductivity is therefore proportional to density.

Electrochemical delithiation.—The sintered pellets were polished to thicknesses of 0.30 to 0.80 mm. Delithiation was performed in a Swagelok-type electrochemical cell using lithium metal foil as the counter electrode, the NMC pellet as the working electrode, and a liquid electrolyte mixture containing 1 M $LiPF_6$ in 1:1 by mole of ethylene carbonate/diethyl carbonate (EC/DEC). One side of the polished pellets was burnished with a thin layer of graphite to form good electrical contact with the metal current collectors in the cells. A Celgard separator (Charlotte, NC, USA) was used to separate the electrodes. A charging current equivalent to C/200 and/or C/400 rate was applied

[z]E-mail: ychiang@mit.edu

Table I. Summary of techniques and cell configurations used to elucidate electronic and ionic conductivity, and the ion diffusivity, as a function of temperature and/or Li-content.

Probed	Technique	Cell configuration	Transport properties as a function of
Electronic conductivity	EIS - AC	Ag/NMC/Ag	Temperature, Li-content
	EIS - DC	Ag/NMC/Ag	Temperature, Li-content
Ionic conductivity	EIS - AC	Li/PEO/NMC/PEO/Li	Temperature
	EIS - DC	Li/PEO/NMC/PEO/Li	Temperature
Ion diffusivity	EIS - AC and DC	Li/PEO/NMC/PEO/Li	Temperature
	Depolarization	Li/Separator/(electrolyte)/ NMC/current collector	Li- content

Abbreviations: EIS: Electrochemical Impedance Spectroscopy, AC: Alternating Current, DC: Direct Current, GITT: Galvanostatic Intermittent Titration Technique, NMC: $LiNi_{0.50}Mn_{0.20}Co_{0.30}O_2$ or $LiNi_{0.33}Mn_{0.33}Co_{0.33}O_2$, PEO: polyethylene oxide.

continuously or intermittently using a Bio-logic SA France Model VMP3 instrument (Claix, France). After electrochemical delithiation to the desired compositions, the cells were allowed to relax at open circuit voltage conditions, disassembled and the pellets were washed with acetone and pure EC/DEC solvent, and heated at 120°C in an inert atmosphere for at least 24 h in order to homogenize the lithium distribution. The pellets were again polished lightly on both sides to remove any surface lithium salt.

Electronic conductivity measurement.—The as-sintered lithiated and partially delithiated pellets were painted with silver paste on both surfaces forming the symmetric cell configuration Ag|NMC|Ag. The pellets were subsequently heated at 120°C overnight in order to remove the organic solvent in the silver paint. The Ag|NMC|Ag cells were placed in battery coin cell holders with supporting stainless steel disks on both sides of the pellet. Direct current polarization technique (DC) as well as electrochemical impedance spectroscopy (EIS) was employed to measure the electrical conductivity of the samples, using the Bio-logic VMP3 instrument, in the frequency range 200 kHz–0.5 Hz. The measurements were performed at temperatures from 25–100°C using a VWR temperature controller. The sample temperature was measured using a thermocouple.

Ionic transport measurements.—The ionic diffusivity and conductivity of the fully lithiated, starting NMC was measured by direct current (DC) polarization and by electrochemical impedance spectroscopy (EIS). EIS was measured over the frequency range 200 kHz–10 μHz at AC amplitude of 10 mV, and as a function of temperature. Doped polyethylene oxide (PEO) was used as an electron-blocking, lithium-conducting electrode layer. The measurements were performed in the symmetric cell configuration Li|PEO|NMC|PEO|Li in a Swagelok-type cell. The PEO membrane was fabricated by mixing PEO powder (from Scientific Polymer Products, Inc., Mw 4,000,000) and LiI (from Aldrich, 99.99%) in a 6:1 molar ratio in dry acetonitrile. Details of preparation can be found elsewhere.[24]

In order to measure ion diffusivity as a function of lithium content, DC polarization/depolarization measurements were performed on thin sintered NMC pellets (0.26–0.30 mm thickness and 0.219–0.158 cm^2 surface area), using Swagelok-type cells. The same cell preparation procedure and components as described above for electrochemical delithiation were used. A charging current equivalent to C/200 and/or C/400 rate were applied for 10 h, after which the cell was relaxed at open circuit voltage (OCV) conditions for at least 25 h to reach the steady state OCV. Lithium ionic diffusivity was derived from the voltage relaxation vs time (depolarization process). The diffusion length was assumed throughout to be one half the sample thickness.

Results and Discussion

Electronic conductivity.—The impedance spectra of as-sintered lithiated NMC_{523} measured at selected temperatures in the symmetric ion-blocking cell configuration, Ag|NMC|Ag are shown in Figure 1a. Nearly perfect semicircles are obtained in the temperature range 25–100°C and in the frequency range 2×10^6–5×10^{-1} Hz. Similar impedance spectra were observed for the partially delithiated NMC_{523} and NMC_{333}. The impedance spectra were evaluated with the ideal equivalent circuit shown in Figure 1b. For temperature-dependent measurements, impedances were measured during both heating and cooling. The capacitance (C) values can be calculated from the fitting parameters Q and n according to $C = (R^{1-n}Q)^{1/n}$ where Q is a constant phase element and n is a measure of the degree of depression of an arc (here n is usually in the range of 0.96–0.90 depending on the temperature and degree of delithiation). Derived capacitance values are ~5 $\times$ 10^{-11}F and thus confirm that the observed impedance responses originate from the bulk (grains) of the samples (i.e., the values are

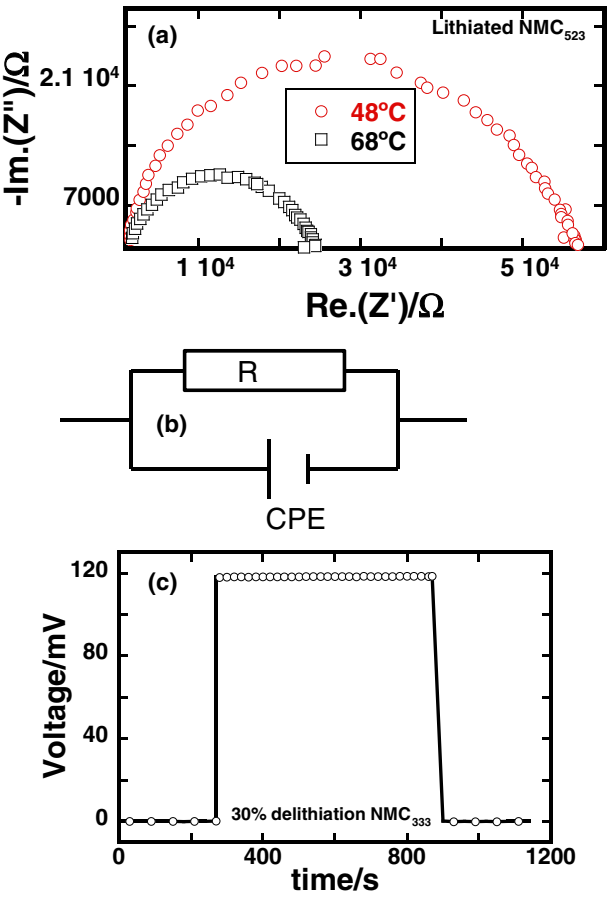

Figure 1. (a) Impedance spectra of as-sintered fully lithiated NMC_{523} ($LiNi_{0.50}Mn_{0.20}Co_{0.30}O_2$) at two different temperatures measured using the symmetrical cell configuration Ag/NMC/Ag, (b) equivalent circuit used to evaluate the impedance spectra, and (c) time dependent voltage in polarization measurements performed at partially delithiated NMC_{333} ($LiNi_{0.33}Mn_{0.33}Co_{0.33}O_2$) in the same cell configuration under constant applied current.

several orders of magnitude smaller than expected for grain boundary impedance).[25] The absence of any additional polarization process (i.e., a second semicircle) at low frequencies for all samples indicates that this conduction is predominantly due to electronic carriers. In order to substantiate this observation, DC polarization and depolarization measurements were performed for lithiated and partially delithiated NMC samples using the same cell configuration as for impedance spectroscopy. Figure 1c is representative of a typical DC measurement on a NMC_{333} sample. During application of a constant current the voltage increases in a step-function manner to a constant value, and decays as a step-function upon switching off the applied current. Such behavior is indicative of an electronically dominated conduction process since in the case of significant contributions from ionic motion, slower relaxation of voltage upon polarization and depolarization with rate constants determined by lithium diffusion D_{Li} are expected.[26–29]

The electronic conductivities of the lithiated and partially delithiated NMC_{523} and NMC_{333} are plotted in Figures 2a and 2b as a function of inverse temperature. The conductivities of the partially delithiated samples measured at a given temperature increase monotonically with increasing delithiation (Figure 2c, for measurements at 30°C). Over the measured compositional range, the electrical conductivity shows thermally-activated behavior. The values of activation energy, calculated using an Arrhenius law, range from 0.42–0.05 eV (±0.03 eV) as shown in Figures 2a and 2b, and are similar in magnitude to the value reported by Saadoune and Delmas[30] for $Li_xNi_{0.80}Co_{0.20}O_2$. These are typical values for the migration of a small polaron, as is generally observed in mixed-valence systems.[31] It has been reported that Co is less prone to oxidize from the trivalent to tetravalent state in the presence of Ni.[32] The electronic configurations of Co^{3+}, Ni^{2+} and Ni^{4+} have the (t_2) orbital filled in each case. As a result, electron delocalization is unlikely. The increase in electronic conductivity is associated with the presence of mixed Ni^{3+}/Ni^{4+} valence states resulting from delithiation, which leads to hole formation in the narrow (Ni^{4+}/Ni^{3+}) band. It is seen from Figures 2a–2c that upon initial delithiation, the sample exhibits a sharp rise in electronic conductivity. Then the slope decreases, although another slight upward inflection appears between $x = 0.5$ and 0.75. In our previous study of transport in NCA, we observed a sharp rise of conductivity beyond 60% delithiation.[33] This was explained as the oxidization of a small amount of cobalt from the trivalent to tetravalent state at this delithiation level.[33] It seems that there may also be a small degree of cobalt oxidation in NMC since the conductivity pattern is similar to NCA. We were not able to measure the electronic conductivity beyond 75% delithiation in the NMC samples, as the samples became too fragile to assemble into cells, due to the intercalation-induced dimensional changes at the crystallite level. It is also seen in Figure 2 that the starting NMC_{523} exhibits higher electronic conductivity than the starting NMC_{333}, although after 30% delithiation both have similar electronic conductivity. The initial higher conductivity of the NMC_{523} may be due to the higher Ni content, since Ni is considered an active conduction site which may facilitate electron hopping.

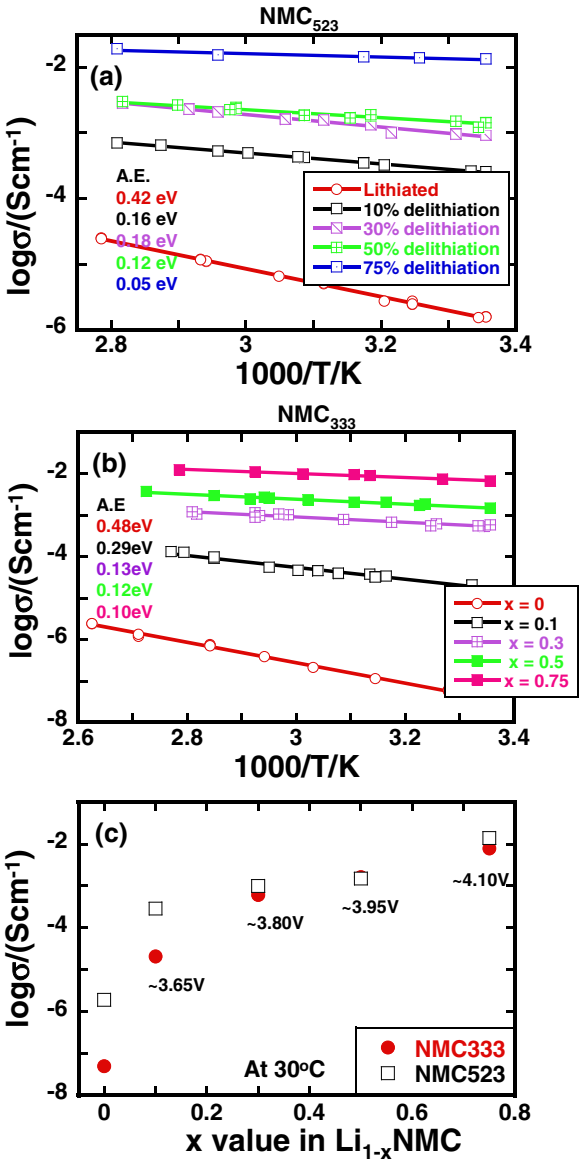

Figure 2. Electronic conductivity of lithiated and partially delithiated (a) NMC_{523} ($LiNi_{0.50}Mn_{0.20}Co_{0.30}O_2$) and (b) NMC_{333} ($LiNi_{0.33}Mn_{0.33}Co_{0.33}O_2$) (as a function of inverse temperature obtain from DC measurement and calculated activation energy using the Arrhenius equation. AC impedance also exhibit same magnitude of conductivity). (c) The electronic conductivity of NMC ($Li_{1-x}NMC$) as a function of x value in $Li_{1-x}NMC$ at 30°C obtained from DC measurement. After electrochemical delithiation to the desired compositions, the cells were allowed to relax under open circuit voltage conditions.

Ionic conductivity by AC impedance.—Interpretation of results for the electron-blocking cells must take into account the temperature dependent ionic conductivity of the PEO blocking layer. Figure 3a shows the impedance spectra of lithiated NMC_{333} measured at 61°C in the cell configuration Li/PEO/NMC/PEO/Li. In contrast to the ion-blocking cells above, these impedance spectra consist of one semicircle at high frequencies (inset of Figure 3a) followed by a Warburg response at low frequencies. The high frequency semicircle represents the total resistance to electronic and ionic motion including contributions from the bulk conductivity of PEO. The Warburg response is indicative of stoichiometric polarization owing to blocking of electrons. In order to obtain the ionic conductivity and diffusivity, the impedance spectra were fitted with the equivalent circuit as shown in Figure 3b using Zview software. The lower frequency Warburg response provides the ionic resistance, and the relaxation frequency of the Warburg response provides the relaxation time, from which we obtained ionic diffusivity as shown in the inset of Figure 3a. Qualitatively similar impedance spectra were observed for NMC_{523}; however, at temperatures below 60°C the frequency range is not sufficiently wide to obtain the relaxation frequency. Hence, for the lower temperatures, the model fit to lower frequencies was extrapolated to reach the relaxation frequency. We were not able to measure at temperatures higher than 60°C due to melting of the PEO film, which tended to short circuit the cell. The activation energy for ionic conductivity and diffusivity could not be reliably extracted due to the narrow measurement temperature range. The ionic conductivity and diffusivity of NMC_{333} and NMC_{523} are compared in Table II at two different temperatures between 50–60°C for each composition. This is to our knowledge the first measurement of these ion transport parameters in any pure phase NMC samples. It is seen from Table II that ionic diffusivity is higher than ionic conductivity at the same temperature. Given the predominant elec-

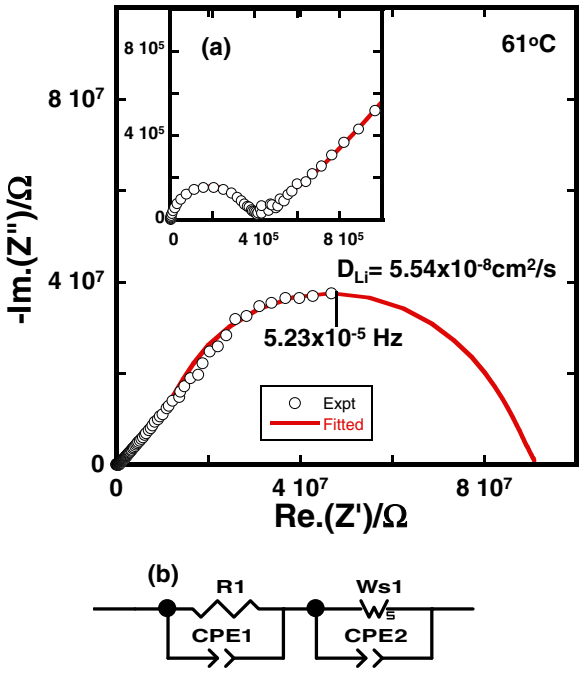

Figure 3. (a) Impedance spectra of NMC_{333} ($LiNi_{0.33}Mn_{0.33}Co_{0.33}O_2$) obtained at 61°C from the electron blocking cell configuration Li/PEO/NMC/PEO/Li. Inset shows the enlarged high frequency spectra. Similar impedance spectra were measured for NMC_{523} ($LiNi_{0.50}Mn_{0.20}Co_{0.30}O_2$) (b) Equivalent circuit used to fit the impedance spectra.

tronic conductivity, the Li^+ diffusivity (D_{Li}) should have the form $D_{Li} \propto \sigma_{ion}(\frac{x_{ion}}{C_{ion}} + \frac{x_{eon}}{C_{eon}})$ where x_{ion} and x_{eon} refer to the contributions due to trapping of ionic and electronic carriers (values of x_{ion} and x_{eon} being between zero and one) and c_{ion}, c_{eon} denote the ionic and electronic carrier concentrations.[34] Since the measurement was performed at relatively high temperature, there should be minimal charge carrier trapping. That is, charge carrier association-dissociation is not prominent in the measured temperature range, and x_{ion} and x_{eon} both reach their limiting value of unity. In the intrinsic dilute defect limit, $c_{ion} \gg 1$, the ionic diffusivity should be higher than the ionic conductivity according to above equation, as is observed in Table II.

Ionic diffusivity by steady state polarization/depolarization.— DC polarization/depolarization measurements were also performed using electronically blocking cell arrangements in order to substantiate the results obtained from the impedance measurements. These measurements were not performed at low temperature due to the excessively long times required to reach steady state (also observed in AC impedance). Figure 4a shows the time dependence of the polarization/depolarization voltage. The voltage immediately jumps from zero to $IR_{el}R_{ion}/(R_{el} + R_{ion})$ where R_{ion} and R_{el} are the resistances due to Li ion and electronic carriers. With increasing time, the partial current of the blocked electrons decreases and eventually vanishes. A

Table II. Ionic conductivity and diffusivity in NMC_{333} and NMC_{523} at two sets of temperatures measured in electron blocking cells using AC and DC techniques.

T/°C	Diffusivity/ cm^2s^{-1}	Conductivity/ Scm^{-1}	Composition	Technique
51	2.2×10^{-8}	9.1×10^{-9}	NMC_{333}	AC
61	5.5×10^{-8}	2.1×10^{-8}		
50	1.5×10^{-8}	8.7×10^{-9}	NMC_{523}	AC
60	4.5×10^{-8}	9.3×10^{-9}		
50	6.1×10^{-9}	3.7×10^{-9}	NMC_{333}	DC (polarization)
50	7.6×10^{-9}	3.7×10^{-9}	NMC_{333}	DC (depolarization)

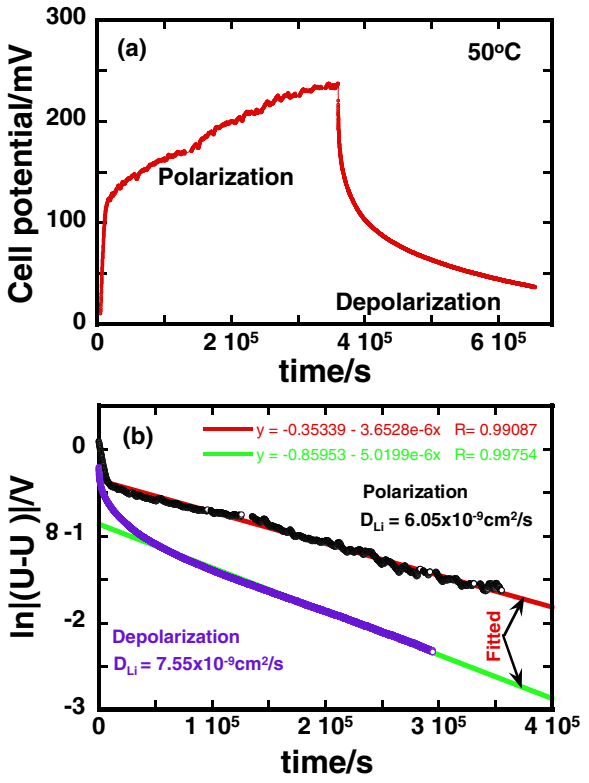

Figure 4. (a) Time dependent of DC polarization voltage at ~50°C obtained from the electron blocking cell Li/PEO/NMC/PEO/Li. (b) Polarization and depolarization results are fitted with Eq. 1 in order to obtain ionic conductivity and diffusivity.

steady state is then observed (voltage being IR_{ion}) during which the total current is carried only by the unblocked ions. The ionic conductivity can be obtained from this ionic resistance. The relaxation time of the polarization process is τ^{δ}, which provides the chemical diffusion coefficients D_{Li} (via $\tau^{\delta} = L^2/(\pi^2 D_{Li})$. It should be noted that owing to the internal concentration profiles, σ_{ion} and D_{Li} are averaged over a Li composition range, corresponding to a polarization voltage of 250 mV. The behavior of the depolarization was analogous to that during polarization. Owing to the relatively high diffusion coefficients, a steady state cell voltage was reached during polarization at ~50°C. The long-time polarization voltage (for $t > \tau^{\delta}$) depends on time according to:[26–28]

$$U_{ion} = \left[(i_p L)/\sigma\right] + \left(\frac{\sigma_{el}}{\sigma}\right)\left[\frac{i_p L}{\sigma_{ion}}\right]\left\{1 - (8/\pi^2)\, exp\left[-\left(\frac{t}{\tau^{\delta}}\right)\right]\right\} \quad [1]$$

A plot of $\ln|U(t) - U(t = \infty)|$ vs. t should generate a straight line with a slope of $\tau^{\delta} \propto (\frac{1}{D_{Li}})$. Figure 4b shows that this relationship is followed to $R > 0.99$ over a wide time interval. Diffusivity and ionic conductivity data derived from the DC measurement are compared in Table II with the AC data, where it is seen that the two are in good agreement.

Lithium ion diffusivity as a function of lithium concentration from depolarization measurements.—Figure 5a shows an example of the cell voltage vs. time during the stepwise galvanostatic titration of fixed amounts of lithium from the NMC sample. A lithium concentration gradient is developed across the sample during titration. After each delithiation step, the cell is allowed to relax in the OCV condition, and the cell voltage slowly reaches steady state, corresponding to removal of the lithium concentration gradient. Lithium ion diffusivity data derived from the relaxation of the cell voltage, i.e. the depolarization process, using Eq. 1 is shown in Figure 5b. It is seen that the depolarization cell voltage can be fitted very well with Eq. 1.

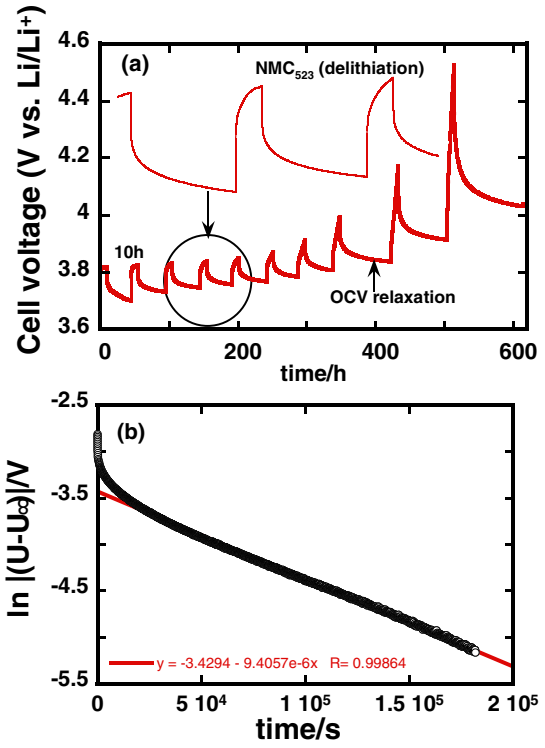

Figure 5. (a) Time dependent cell voltage measured on the NMC_{523} ($LiNi_{0.50}Mn_{0.20}Co_{0.30}O_2$) plate by titrating a fixed amount of lithium and holding at open circuit conditions. (b) Fit of the depolarization cell voltage to Eq. 1 in order to extract the chemical diffusivity of lithium ion and similar measurements were performed for NMC_{333} ($LiNi_{0.33}Mn_{0.33}Co_{0.33}O_2$).

The room-temperature lithium ion diffusivity for NMC_{333} and NMC_{523} obtained from these measurements are plotted in Figure 6 as a function of lithium content. Although data for both compositions have similar trends, NMC_{523} exhibits the higher diffusivity throughout the lithium content range. This may be due to the higher Mn^{4+} concentration in NMC_{333}, which may create a stronger interaction with lithium ions than in NMC_{523} and reduce lithium ion mobility. Note that the ionic diffusivity varies with x by almost an order of magnitude in NMC_{333}, and somewhat less in NMC_{523}. However, the ionic diffusivity is, even at its minimum value near $x = 0.5$, more than 10^7 lower than the electronic conductivity (comparing Figures 2c and 6). In addition, the ionic diffusivity shows an inverse relationship to the unit cell parameters, which we also found to be the case for NCA.[33] Extensive structural and lattice parameter studies as a function of lithium content NMC[12,17] show a systematic increase of unit cell dimensions with increasing delithiation, whereas we observe a decrease of ionic diffusivity with delithiation. This is surprising, and is counter to the

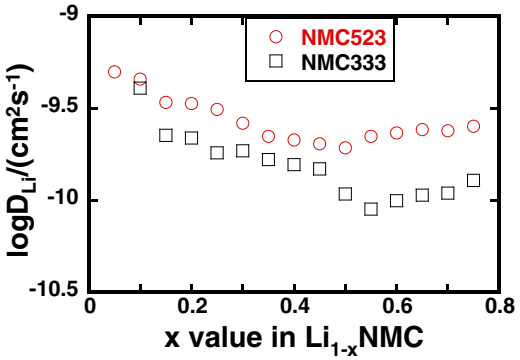

Figure 6. Comparison of diffusivity of NMC_{333} and NMC_{523} as a function of lithium content at room temperature obtained from depolarization experiments shown in Figure 5a.

expectation that a c-axis expansion corresponding to an increase in the Li slab distance lowers the activation energy for migration and should therefore increase the Li diffusion coefficient.[35,36] The dependence of ion diffusivity on Li vacancy concentration x is consistent with a defect chemical model where between $x = 0$ and $x = 0.5$, diffusivity is dependent on interstitial concentration and therefore decreases with increasing vacancy concentration through a Frenkel point-defect equilibrium. However, we believe that the increase in diffusivity for $x > 0.5$ is due to extrinsic effects whereby electrochemically-induced fracture, also known as "electrochemical shock" by analogy with thermal shock,[37–39] creates microcracks that are then filled with liquid electrolyte and provide fast transport paths. NMC, like other "layered" oxides, exhibits anisotropic chemical expansion that generates misfit stresses between crystallites, the magnitude of which are state-of-charge rather than C-rate dependent.[38,39] As a result, the effective diffusion length for ion transport decreases, leading to an apparent increase in diffusivity.

We know of no other pure-phase diffusion data for NMC to compare with the present results. For NMC_{333}, however, Wu et al.[19] reported a monotonic increase in chemical diffusion coefficient with lithium content for NMC_{333}, based on GITT measurements of composite electrodes. The diffusivity data ranged from $\sim 10^{-12}$ to $\sim 10^{-10}$ $cm^2\ s^{-1}$ over the entire Li-compositional window.[19] Our diffusivity data are higher, and lie between 5.0×10^{-10} to 1.3×10^{-10} to $cm^2\ s^{-1}$ over the lithium content from x = 0.05 to x = 0.75. In contrast, Hao[20] reported an almost constant lithium diffusion coefficient of $\sim 10^{-10}$ $cm^2\ s^{-1}$ for NMC_{333} over the cell voltage range 3.5 V to 4.3 V. Gu et al.[21] found a much low diffusivity of $\sim 10^{-14}$ $cm^2\ s^{-1}$ using the CV method in fully lithiated NCM_{523}. We believe that extrinsic factors may contribute to some extent in these previous results due to the composite samples used, and that none may represent the pure single phase transport behavior. A summary of the diffusivity data from the present work, at several specific compositions and temperatures, are compared with previous literature results in Table III.

Table III. Comparison of lithium ion diffusivity of NMC_{333} and NMC_{523} from the present work with available literature data.

Technique Used	T/°C	Composition	Diffusivity (cm^2/s)	Reference
AC	60	$LiNi_{0.50}Mn_{0.20}Co_{0.30}O_2$ (NMC_{523})	4.5×10^{-8}	This study
AC	61	$LiNi_{0.33}Mn_{0.33}Co_{0.33}O_2$ (NMC_{333})	5.5×10^{-8}	This study
DC	50	$LiNi_{0.33}Mn_{0.33}Co_{0.33}O_2$ (NMC_{333})	7.6×10^{-9}	This study
Depolarization	25	$Li_{0.90}Ni_{0.33}Mn_{0.33}Co_{0.33}O_2$ (NMC_{333})	4.1×10^{-10}	This study
Depolarization	25	$Li_{0.25}Ni_{0.33}Mn_{0.33}Co_{0.33}O_2$ (NMC_{333})	1.3×10^{-10}	This study
Depolarization	25	$Li_{0.90}Ni_{0.50}Mn_{0.20}Co_{0.30}O_2$ (NMC_{523})	4.6×10^{-10}	This study
Depolarization	25	$Li_{0.25}Ni_{0.50}Mn_{0.20}Co_{0.30}O_2$ (NMC_{523})	2.5×10^{-10}	This study
GITT	25	$LiNi_{0.33}Mn_{0.33}Co_{0.33}O_2$ (NMC_{333})	$\sim 10^{-12}$	19
GITT	25	$Li_{0.25}Ni_{0.33}Mn_{0.33}Co_{0.33}O_2$ (NMC_{333})	$\sim 10^{-10}$	19
GITT	25	$LiNi_{0.33}Mn_{0.33}Co_{0.33}O_2$ (NMC_{333})	$\sim 10^{-10}$	20
CV	25	$LiNi_{0.33}Mn_{0.33}Co_{0.33}O_2$ (NMC_{333})	$\sim 5 \times 10^{-14}$	21
CV	25	$LiNi_{0.33}Mn_{0.33}Co_{0.33}O_2$ (NMC_{333})	$\sim 3 \times 10^{-10}$	23

Conclusions

Electronic and lithium ionic transport in NMC have been measured using ion and electron blocking cell configurations and AC and DC techniques. NMC exhibits semiconducting electronic conductivity over the range of lithium concentrations from $x = 0.0$ to 0.75. Starting from the fully lithiated state, the electronic conductivity increases with increasing delithiation, which is attributed to Ni^{3+}/Ni^{4+} multivalency, and rises especially sharply over the initial 10% of delithiation. There is a second upward inflection at about 75% delithiation, which may be due to the onset of Co^{3+}/Co^{4+} multivalency. The ion diffusivity as a function of lithium concentration decreases with delithiation up to at least $x = 0.5$. Since the unit cell parameters in published literature show the opposite trend with a maximum at $x = 0.5$, the observed diffusivity behavior is counter to expectations for ion migration energy as a function of *c*-axis dimensions, and suggests more subtle cation ordering effects that remain to be resolved. From the magnitude of the electronic and ionic transport parameters across the measured range of Li concentration, it is concluded that chemical diffusion is always limited by lithium ion transport rather than electronic conductivity. From the reported ion transport coefficients, kinetic requirements such as the particle size necessary for particular charge/discharge times can be readily calculated.

Acknowledgments

This work was supported as part of the North East Center for Chemical Energy Storage (NECCES), an Energy Frontier Research Center funded by the U.S. Department of Energy, Office of Science, Basic Energy Sciences under Award # DE-SC0012583.

References

1. V. K. Etacheri, R. Marom, R. Elazari, G. Salitra, and D. Aurbach, *Energy Environ. Sci.*, **4**, 3243 (2011).
2. J. Cabana, H. Zheng, A. K. Shukla, C. Kim,V. S. Battaglia, and M. Kunduraci, *J. Electrochem. Soc.*, **158**, A997 (2011).
3. R. Koksbang, J. Barker, H. Shi, and M. Y. Saidi, *Solid State Ionics*, **84**, 1 (1996).
4. J. L. Lei, F. McLarnon, and R. Kostecki, *J. Phys. Chem. B*, **109**, 952 (2005).
5. A. D. Epifanio, F. Ronci, V. R. Albertini, E. Traversa, and B. Scrosati, *Phys. Chem. Chem. Phys.*, **3**, 4399 (2001).
6. C. H. Lu and H. C. Wang, *J. Mater. Chem.*, **13**, 428 (2003).
7. A. Kinoshita, K. Yanagida, A. Yanai, Y. Kida, A. Funahashi, T. Nohma, and I. Yonezu, *J. Power Sources*, **102**, 283 (2001).
8. A. Ueda and T. Ohzuku, *J. Electrochem. Soc.*, **141**, 2010 (1994).
9. J. Cho, G. Kim, and H. S. Lim, *J. Electrochem. Soc.*, **146**, 3571 (1999).
10. C. C. Chang, N. Scarr, and P. N. Kumta, *Solid State Ionics*, **112**, 329 (1998).
11. R. V. Chebiam, F. Prado, and A. Manthiram, *J. Electrochem. Soc.*, **148**, A49 (2001).
12. N. N. Sinha and N. Munichandraiah, *ACS Appl. Mater. & Interfaces* **6**, 1241 (2009).
13. N. N. Sinha and N. Munichandraiah, *J. Electrochem. Soc.* **157**, A647 (2010).
14. H. Sclar, D. Kovacheva, E. Zhecheva, R. Stoyanova, R. Lavi, G. Kimmel, J. Grinblat, O. Girshevitz, F. Amalraj, O. Haik, E. Zinigrad, B. markovsky, and D. Aurbach, *J. Electrochem. Soc.*, **156**, A938 (2009).
15. F. Wu, M. Wang, Y. Su, L. Bao, and S. Chen, *J. Power Sources*, **195**, 2362 (2010).
16. A. M. A. Hashem, A. E. Abdel-Ghany, A. E. Eid, J. Trottier, K. Zaghib, A. Mauger, and C. M. Julien, *J. Power Sources*, **196**, 8632 (2011).
17. K. C. Kam, A. Mehta, J. T. Heron, and M. M. Doeff, *J. Electrochem. Soc.*, **159**, A1383 (2012).
18. Y. Gao, M. V. Yakovleva, and W. B. Ebner, *Electrochem. Solid State Lett.*, **1**, 117 (1998).
19. S.-L. Wu, W. Zhang, X. Song, A. K. Shukla, G. Liu, V. Battaglia, and V. Srinivasan., *J. Electrochem. Soc.*, **159**(4), A438 (2012).
20. L. Hao, master thesis, City University of Hong Kong (2010).
21. Y.-J. Gu, Q.-G. Zhang, Y.-B. Chen, H.-Q. Liu, J.-X. Ding, Y.-M. Wang, H.-F. Wang, L. Chen, M. Wang, S.-W. Fan, Q.-F. Zang, and X.-L. Yang, *J. Alloys and Compounds*, **630**, 316 (2015).
22. K. A. Seid, J. C. Badot, O. Dubrunfaut, M. T. Caldes, N. Stephant, L. Gautier, D. Guyomardcd, and B. Lestriezcd, *Phys. Chem. Chem. Phys.*, **15**, 19790 (2013).
23. X. Li, J. Liu, M. N. Banis, A. Lushington, R. Li, M. Cai, and X. Sun, *Energy Environ. Sci.*, **7**, 768 (2014).
24. Y. Liu, S. Gorgutsa, C. Santato, and M. Skorobogatiy, *J. Electrochem. Soc.*, **159**(4), A349 (2012).
25. F. S. Baumann, PhD thesis "Oxygen reduction kinetics on mixed conducting SOFC model cathodes" Stuttgart University press, 2006, page 33.
26. C. Wagner, *Proc. 7th Meeting Int. Comm. on Electrochem. Thermodynamics and Kinetics*, Lindau 1955, Butterworth, London, 1957.
27. I. Yokota, *J. Phys. Soc. Japan.*, **16**, 2213 (1961).
28. J. Maier, *Physical Chemistry of Ionic Materials: Ions and Electrons in Solids*, Wiley, Chichester (2004).
29. R. Amin, J. Maier, P. Balaya, D. P. Chen, and C. T. Lin, *Solid State Ionics.*, **178**, 1683 (2008).
30. I. Saadoune and C. Delmas, *J. Solid State Chem.*, **136**, 15 (1998).
31. T. Maxisch, F. Zhou, and G. Ceder, *Physical Review B* **73**, 104301 (2006).
32. D. Carlier, M. Menetrier, and C. Delma, *J. Mater. Chem.*, **11**, 594 (2001).
33. R. Amin, D. B. Ravnsbæk, and Y.-M. Chiang. *J. Electrochem. Soc.*, **162**(7), A1163 (2015).
34. J. Maier, *J. Am. Ceram. Soc.*, **76**, 1212 (1993).
35. A. Van der Ven and G. Ceder, *Electrochem. and Solid State. Lett.*, **3** (7), 301 (2000).
36. K. Kang and G. Ceder, *Phys. Rev. B*, **74**(9), 094105 (2006).
37. W. Woodford, Y.-M. Chiang, and W. C. Carter, *J. Electrochem. Soc.*, **157**(10), A1052 (2010).
38. W. H. Woodford, W. C. Carter, and Y.-M. Chiang, *Energy and Environmental Science*, **5**, 8014 (2012).
39. W. H. Woodford, Y.-M. Chiang, and W. C. Carter, *J. Electrochem. Soc.*, **160**(8), A1286 (2013).

Journal of The Electrochemical Society, **163** (10) X7-X7 (2016)
0013-4651/2016/163(10)/X7/1/$33.00 © The Electrochemical Society

Erratum: Characterization of Electronic and Ionic Transport in $Li_{1-x}Ni_{0.33}Mn_{0.33}Co_{0.33}O_2$ (NMC_{333}) and $Li_{1-x}Ni_{0.50}Mn_{0.20}Co_{0.30}O_2$ (NMC_{523}) as a Function of Li Content [*J. Electrochem. Soc.*, 163, A1512 (2016)]

Ruhul Amin[a,b] and Yet-Ming Chiang[a]

[a]*Department of Materials Science and Engineering, Massachusetts Institute of Technology (MIT), Cambridge, Massachusetts 02139, USA*
[b]*Qatar Environment and Energy Research Institute, Hamad Bin Khalifa University, Qatar Foundation, Doha, Qatar*

Throughout this paper, $Li_{1-x}Ni_{0.50}Mn_{0.20}Co_{0.30}O_2$ should be $Li_{1-x}Ni_{0.50}Mn_{0.30}Co_{0.20}O_2$ and NMC_{523} should be NMC_{532}.